Modeling the contact between a rolling sphere and a compliant ground plane

Morteza Azad and Roy Featherstone
Australian National University, Australia
morteza.azad@anu.edu.au, roy.featherstone@anu.edu.au

Abstract

In this paper a complete 3D contact model is presented. This model has nonlinearity in determining both normal and friction forces. A new nonlinear normal force model is introduced and the differences between this new model and previous ones are described. Also, the characteristics of this model are discussed and compared with the classical models and empirical results. For calculating the friction force, a new nonlinear model which is able to calculate presliding displacement and viscous friction is presented. It is shown that this model allows us to keep track of all the energy in the system and therefore, supports an energy audit.

Also, the rolling motion of a sphere on a compliant ground plane is simulated, and the results are presented. Rolling motion is an integral part of simulating the general 3D motion of a robot's foot while in contact with the ground.

1 Introduction

Robotic systems usually make contact with their environment during execution of their tasks. So modeling the contact is an inevitable part of every study in this field. In particular, in the case of legged robots, modeling the contact between the robot's feet and the ground is one of the most important parts of the study. Also, it is desirable to find the amount of energy dissipated during the contact because minimizing the energy consumption might be one of the objectives of designing legged robots.

As we know, two major forces appear in each contact: normal and friction forces, and so it is desirable to have a complete model for the contact which is able to model both normal and friction forces. In this paper, we look at the contact models which are mentioned in the literature and try to provide a full 3D model for calculating contact forces and determining the amount of dissipated energy.

For modeling the normal force, there are two general types: rigid and compliant models [Gilardi and Sharf, 2002]. However, there are two major problems with rigid models: first, some cases arise in which no solution or multiple solutions exist, and second, energy conservation principles may be violated during frictional impacts [Gilardi and Sharf, 2002]. On the other hand, the advantage of compliant models is that by using them, the normal force will be a function of local indentation, and it would be possible to compute the normal force during the contact.

Some researchers have used the compliant model for determining the normal force between a sphere and a compliant plate, instead of the robot's foot and the ground, and have derived some equations for calculating the normal force [Hunt and Crossley, 1975], [Marhefka and Orin, 1999], [Lankarani and Nikravesh, 1990] and [Falcon *et al.*, 1998]. Almost all of them have used Hertz's theory [Johnson, 1977] to predict the normal force with different types of damping terms. In this study, we are going to use a different approach, and of course end up with a new compliant contact model which is different from those classical methods.

Also, many efforts have been made by researchers in modeling the friction force, such as Dupont et al. [2000], Haessig and Friedland [1991], Bliman and Sorine [1995], Dupont et al. [2002], Dahl [1968] and deWit at al. [1995], most of which are reviewed by Olsson et al. [1998]. In fact, friction is a more complicated phenomenon than contact, and many effects are included in friction. Armstrong-Hélouvry et al. [1994] have introduced a nearly complete model which is called the seven parameter friction model. This model is able to capture almost all friction effects, like pre-sliding displacement, coulomb+viscous+stribeck curve, frictional memory and rising static friction. However, this model is too complicated and hard to implement in simulation. Also, there are not enough experimental results for determining the parameters.

In this paper, we are going to introduce a simpler model for friction to capture most common effects like presliding regime and coulomb+viscous friction. In our

model, we have chosen to consider the nonlinearity in the nature of the contact between a sphere and the ground. So, we use a nonlinear friction force instead of linear one in the pre-sliding period.

The purpose of this paper is to look at the contact between a rolling sphere and the compliant ground with focus on the energy dissipation. In modeling the robot's foot with a sphere or a union of spheres, there is a possibility for the sphere to roll over the ground during the contact. So, we must study the rolling motion of the sphere instead of considering the sphere as a point mass.

In section 2 of this paper, the new nonlinear contact model for normal force is described and compared with the classical methods. A nonlinear model for friction force is presented, and its characteristics are discussed in section 3. In section 4, the results of simulation of a rolling sphere on the compliant ground are demonstrated.

2 Nonlinear Normal Force Model

A non-linear equation for the normal force between a sphere and the ground was first introduced by Hunt and Crossley [1975]. They modeled the ground as a nonlinear spring-damper pair at the contact point, and proposed a general form for the normal force, F, exerted on the sphere by the ground, as

$$F = kz^n + \lambda z^p \dot{z}^q \,, \tag{1}$$

where z is the deformation of the ground, $\dot{z}$ is the rate of deformation, k and λ are the coefficients of the spring and damper, respectively, and n, p and q are constant parameters.

Hunt and Crossley [1975], Lankarani and Nikravesh [1990], and Marhefka and Orin [1999] have set the values of these parameters as $n = \frac{3}{2}$ (to get similar results to the Hertz's theory [Johnson, 1977]) and $p = \frac{3}{2}$ and $q = 1$ (to be able to determine the value of λ with respect to k, conveniently) for the contact force between a sphere and a plate:

$$F = kz^{\frac{3}{2}} + \lambda z^{\frac{3}{2}} \dot{z} \,. \tag{2}$$

In this paper, we adopt an alternative model in which the ground is considered to contain a uniform distribution of infinitely many non-linear spring-damper pairs, so that the ground as a whole can be characterized by a stiffness and a damping coefficient per unit area. According to this model, the normal force is given by

$$f = f_K + f_D \,, \tag{3}$$

where f_K and f_D are the forces due to the spring and damper, respectively, and are given by

$$f_K = \int_0^z A(\xi)\, K_A(z-\xi)\, \mathrm{d}\xi \tag{4}$$

and

$$f_D = \int_{A(z)} D_A(\zeta(A))\, \dot{z}\, \mathrm{d}A, \tag{5}$$

where $K_A(z)$ and $D_A(z)$ are the stiffness and damping coefficients per unit area, $A(z)$ is the area of contact expressed as a function of z, and $\zeta(A)$ denotes the *local deformation* at the area element $\mathrm{d}A$. Figure 1 shows how

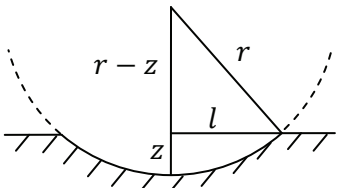

Figure 1: Sideview of Contact Area

the contact area is calculated for a sphere of radius r. We define the contact area to be the area of undeformed ground that makes contact with the sphere, so we have

$$A(z) = \pi l^2 = \pi(2rz - z^2) = 2\pi r z(1 - \frac{z}{2r}) \,. \tag{6}$$

Assuming that $z \ll 2r$, and taking into account that $A(z)$ must be zero for all $z < 0$, we arrive at the following equation for the contact area:

$$A(z) = \begin{cases} 2\pi r z & \text{if } z \geq 0 \\ 0 & \text{otherwise.} \end{cases} \tag{7}$$

In order to conform with Hertz's theory, $K_A(z)$ should be chosen as

$$K_A(z) = \frac{E^*}{2\pi\sqrt{r}}\, z^{-\frac{1}{2}} \,, \tag{8}$$

and E^* is determined by

$$\frac{1}{E^*} = \frac{1-\nu_1^2}{E_1} + \frac{1-\nu_2^2}{E_2} \tag{9}$$

where E_1 and E_2 are the moduli of elasticity, and ν_1 and ν_2 are the poisson ratios of the two contacting surfaces [Johnson, 1977]. Substituting Eqs. (7) and (8) into Eq. (4) gives

$$f_K = \left\{ \begin{array}{cc} \frac{4}{3} E^* \sqrt{r}\, z^{\frac{3}{2}} & \text{if } z \geq 0 \\ 0 & \text{if } z < 0 \end{array} \right\} = K_n z^{\frac{3}{2}} \tag{10}$$

where K_n is a nonlinear spring coefficient that depends only on the mechanical properties of the contacting surfaces, the radius of the sphere and the sign of z (i.e., K_n is defined to be zero if $z < 0$).

Now we assume that $D_A(z)$ has the same relation with z as $K_A(z)$ does. So we can write

$$D_A(z) = \alpha\, z^{-\frac{1}{2}} \tag{11}$$

where α is a constant parameter. Substituting Eqs. (7) and (11) into Eq. (5) gives

$$f_D = \left\{ \begin{array}{cc} 4\pi r\alpha z^{\frac{1}{2}}\dot{z} & \text{if } z \geq 0 \\ 0 & \text{if } z < 0 \end{array} \right\} = D_n z^{\frac{1}{2}}\dot{z}\,, \qquad (12)$$

In analogy with Eq. (1), we can now write our normal force model equation in the form

$$f = K_n z^{\frac{3}{2}} + D_n z^{\frac{1}{2}}\dot{z}\,. \qquad (13)$$

2.1 Coefficient of Restitution

According to experiments reported by Goldsmith [1960] on measuring the coefficient of restitution for a contact between spheres and thick plates, the coefficient of restitution should start from a certain value at high velocities and tend to unity at low impact velocities.

Figure 2 shows the values of the coefficient of restitution at different impact velocities calculated by our model, the classical non-linear model (i.e., Eq. (2)), and the linear model (which is introduced in §11.8 of [Featherstone, 2008]). In every case, gravity is set to zero. (With nonzero gravity, impacts below a threshold velocity do not result in a bounce, implying a coefficient of restitution equal to zero.) This figure indicates that,

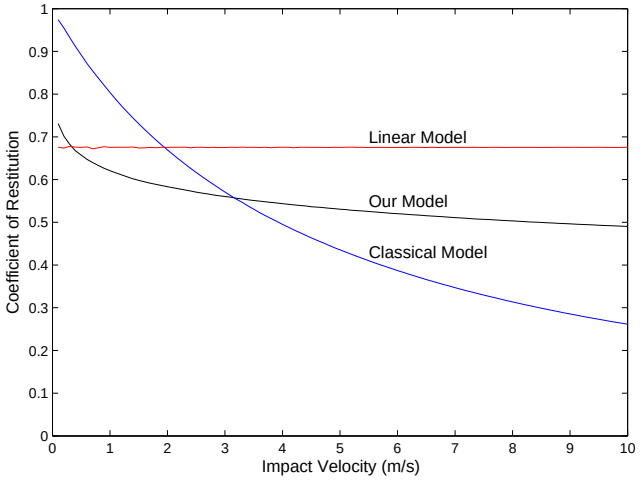

Figure 2: Coefficient of restitution vs. impact velocity calculated by three different models

for the linear model, the coefficient of restitution is constant at all velocities. However, for the nonlinear contact models, this coefficient decreases with increasing impact velocity, with different shapes. This difference can be observed more clearly by changing the scale of the horizontal axis to a logarithmic scale. Figure 3 indicates that our model represents a linear relation between the coefficient of restitution and the logarithm of impact velocity for different values of damping coefficient, D_n, which is

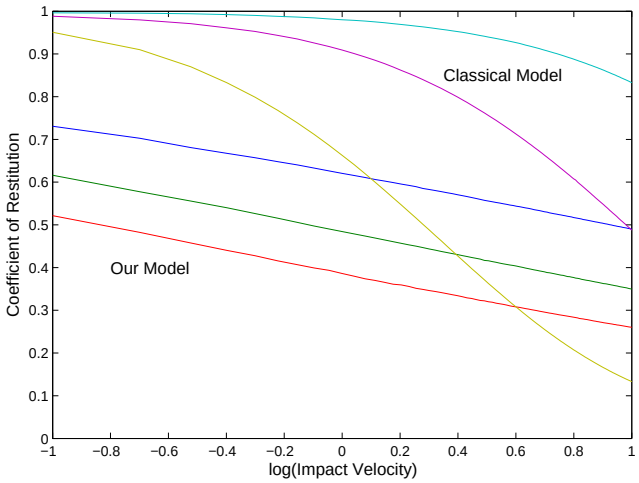

Figure 3: Coefficient of restitution vs. logarithm of impact velocity calculated by the classical model and our model

in contrast with curves that we obtain from the classical model in the logarithmic scale.

In Figure 4 we have compared the calculated values of the coefficient of restitution by our model with empirical results ([Goldsmith, 1960] and [Kuwabara and Kono, 1987]) in a logarithmic scale. By looking at Figure 4 we

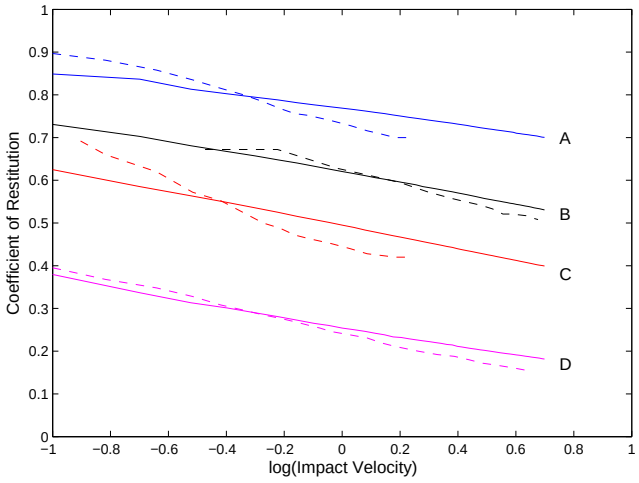

Figure 4: Coefficient of restitution vs. logarithm of impact velocity. Dashed curves show the experimental results and solid curves the calculated values by our model. Results are for the contact between (A) a steel sphere ($r = 1.27$cm) and a cast iron plate, (B) a steel sphere ($r = 1.65$cm) and a cork plate, (C) a steel sphere ($r = 1.27$cm) and a brass plate, and (D) a steel sphere ($r = 1.27$cm) and a cold-worked lead plate.

can conclude that our model fits the empirical results more accurately than the classical model, although the

fit is better in cases (B) and (D) than (A) and (C). In cases (A) and (C), the measured values still show a linear behaviour but their slopes are a bit different from our calculated one.

2.2 Bouncing Simulation

Model Modification for Bouncing

We regard the ground as a first-order dynamical system containing springs and dampers, but no mass. Therefore, if the sphere strikes the ground with enough velocity to bounce, then our model predicts that the sphere will lose contact with the ground before z has fully returned to zero. To avoid having to simulate the recovery of the ground plane after the sphere has lost contact, we accelerate the recovery by adjusting the damping force, as shown below, so that the ground plane rises at the same speed as the sphere, and therefore reaches $z = 0$ at the same time as the bottom of the sphere. This modification does not introduce any kind of error into the model, except one (see Figure 5): if the sphere bounces twice in quick succession, so that the ground has not fully recovered from the first bounce at the time of the second landing, then the modification fails to model the second landing and bounce correctly.

The modified model is defined by Eqs. (3), (10) and the equation below, which replaces Eq. (12):

$$f_D = \max(D_n z^{\frac{1}{2}} \dot{z}, -f_K)\,. \tag{14}$$

This equation ensures that f in Eq. (3) is never negative.

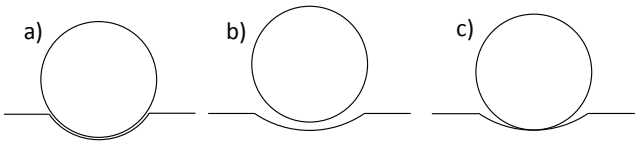

Figure 5: a) end of first bounce b) ground is recovering itself c) re-collision with the ground with undetermined shape.

Normal force vs. Deformation Plot

Figures 6 and 7 show the normal force vs. ground deformation for a sphere with radius $r = 1.65$cm, mass $m = 154$gr and initial velocity of $1\frac{\mathrm{m}}{\mathrm{s}}$, which are simulated by the classical model and our model, respectively.

By comparing these two diagrams, it can be seen that in Figure 7 the normal force reaches zero before z, indicating that our model is able to predict correctly that contact ends before the ground has fully recovered to zero deformation.

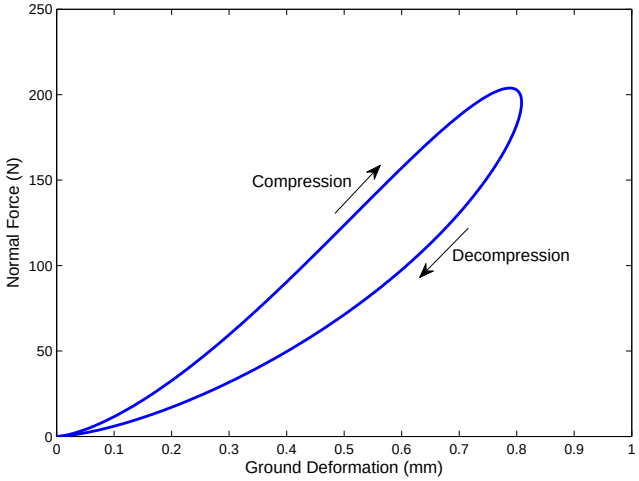

Figure 6: contact force vs. ground deformation for $k = 8.5 \times 10^6$, $\lambda = 3.1 \times 10^6$

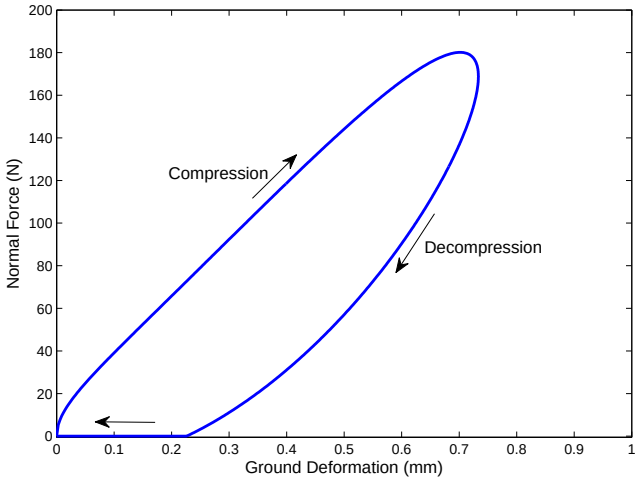

Figure 7: contact force vs. ground deformation for $K_n = 8.5 \times 10^6$, $D_n = 3.1 \times 10^3$

Simulation

The bouncing motion of a sphere with radius $r = 1.65$cm and mass $m = 154$gr is studied in this section. Figure 8 shows the height of the lowest point of the sphere which is released without initial velocity from initial height of 10cm, measured from the bottom of the sphere, and Figure 9 shows the normal force exerted by the ground on the sphere.

Figure 10 shows the contact force exerted on the sphere at the first bounce. It can be seen from this figure that the force is continuous and starts from zero at the beginning of the contact and comes back to zero smoothly. Also it is not sticky (negative) during the contact.

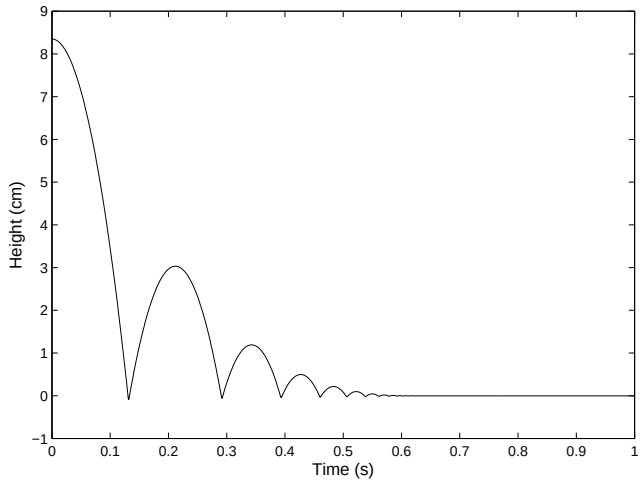

Figure 8: Vertical position vs. time for a bouncing sphere ($K_n = 8.5 \times 10^6$, $D_n = 3.1 \times 10^3$)

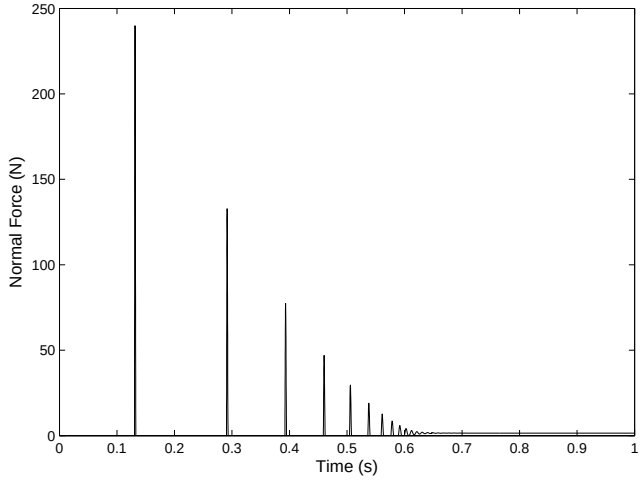

Figure 9: Normal force vs. time for a bouncing sphere ($K_n = 8.5 \times 10^6$, $D_n = 3.1 \times 10^3$)

2.3 Energy Audit

In addition to calculating the contact force, we also implemented an energy audit part in our simulink model for keeping track of all energy in the system. On the basis of energy conservation principle, at any instant of the simulation, the summation of the amount of energy which is dissipated and the amount of energy which is stored in springs and the body itself must be constant:

$$E_{Dissipated} + E_{Springs} + E_{Body} = \text{constant}. \qquad (15)$$

The only dissipative component in this model is the damper, and the amount of energy dissipated by the damper is

$$E_{NDamp} = \int_0^t f_D \dot{z} \mathrm{d}t \ . \qquad (16)$$

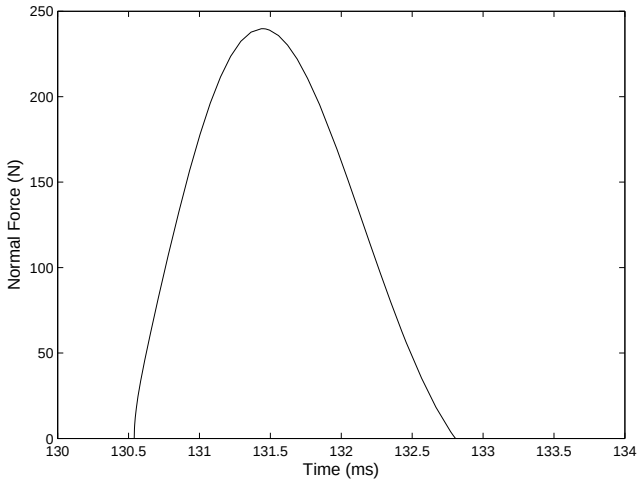

Figure 10: Enlargement of the first bounce in Figure 9

Also, the energy stored in the normal spring can be calculated as

$$E_{NSp} = \int_0^t f_K \dot{z} \mathrm{d}t = \int_0^t K_n z^{\frac{3}{2}} \dot{z} \mathrm{d}t = \frac{2}{5} K_n z^{\frac{5}{2}} \ . \qquad (17)$$

And finally, the amount of energy of the body can be written as the sum of potential and kinetic energy, which is

$$E_{Body} = mgh + \frac{1}{2} m \dot{\boldsymbol{c}}^2 \ , \qquad (18)$$

where h is the height, and $\dot{\boldsymbol{c}}$ is the velocity of the center of mass (COM).

Figure 11 shows the total energy, dissipated energy and stored energy for the bouncing sphere. It can be seen that we have a record of the amount of damped and stored energy at all simulation time.

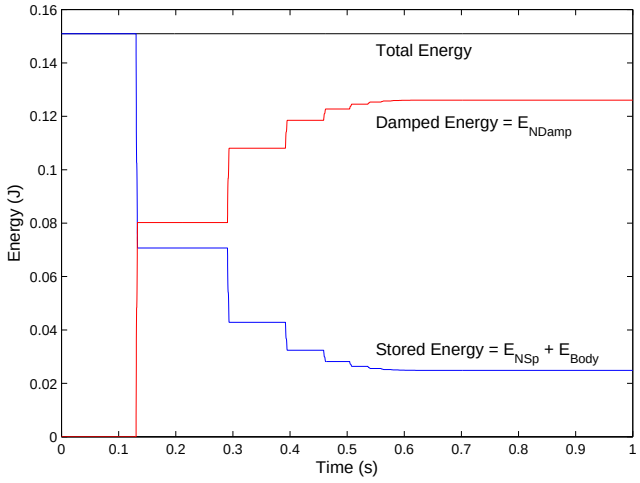

Figure 11: Energy vs. time plot for a bouncing sphere

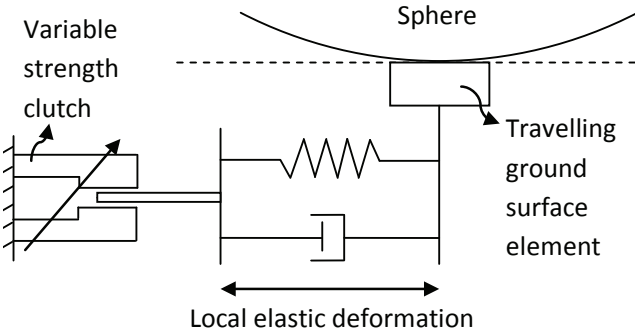

Figure 12: Friction model incorporating presliding through local deformation of a tangential spring and damper, and sliding via a variable-strength clutch that yields at the edge of the friction cone

3 Nonlinear Friction Force Model

In this section, a model for predicting the friction force during the contact period is derived. It is, essentially, a nonlinear, 2D version of the friction model in §11.8 of [Featherstone, 2008]. A physical interpretation of the model is shown in Figure 12. It consists of a spring, a damper and a clutch. The clutch is designed to slip when the ground reaction force reaches the edge of the friction cone. Therefore, the yield force of the clutch depends on the normal force. The major difference between this model and previous friction force models in the literature, is the modeling of stiction force in the presliding regime with a non-linear equation.

To work out the correct friction force, the first step is to work out what the friction force would be if the clutch velocity were zero (i.e., the clutch is not slipping). We call this force $\boldsymbol{f}_{stick}$, and calculate it from

$$\boldsymbol{f}_{stick} = -k_t \boldsymbol{u} - b_t \boldsymbol{V}_{sph}\,, \tag{19}$$

where $\boldsymbol{u}$ is the tangential deformation of the ground at the contact point, $\boldsymbol{V}_{sph}$ is the tangential velocity of the bottom point of the sphere, and k_t and b_t are tangential stiffness and damping coefficients, respectively. As the tangent plane is two-dimensional, $\boldsymbol{f}_{stick}$, $\boldsymbol{u}$ and $\boldsymbol{V}_{sph}$ are all 2D vectors. Similar to the normal spring-damper pair, the coefficients k_t and b_t are functions of the contact area ($A(z)$), and the tangential stiffness and damping coefficients per unit area ($K_A(z)$ and $D_A(z)$). Assuming that the contacting surfaces are isotropic, k_t and b_t are calculated by

$$k_t = \int_{A(z)} K_A(\zeta(A))\,\mathrm{d}A, \tag{20}$$

and

$$b_t = \int_{A(z)} D_A(\zeta(A))\,\mathrm{d}A, \tag{21}$$

(cf. Eqs. (4) and (5)). So, the stiction force can be written as:

$$\boldsymbol{f}_{stick} = -K_t z^{\frac{1}{2}} \boldsymbol{u} - D_t z^{\frac{1}{2}} \boldsymbol{V}_{sph}\,, \tag{22}$$

where K_t and D_t are given by

$$K_t = 2E^* \sqrt{r} \tag{23}$$

and

$$D_t = 4\pi r\,\alpha\,. \tag{24}$$

The correct friction force will either be $\boldsymbol{f}_{stick}$, if it lies inside the friction cone, or else a force lying on the friction cone and having the same direction as $\boldsymbol{f}_{stick}$. We call the latter $\boldsymbol{f}_{slip}$, and calculate it from

$$\boldsymbol{f}_{slip} = \boldsymbol{f}_{stick} \times \frac{\mu F_n}{|\boldsymbol{f}_{stick}|}\,, \tag{25}$$

where μ is the coefficient of friction and F_n is the contact normal force. To avoid a divide-by-zero error, this equation is only calculated if $|\boldsymbol{f}_{stick}| > \mu F_n$. The correct friction force, $\boldsymbol{F}_f$, is now given by

$$\boldsymbol{F}_f = \begin{cases} \boldsymbol{f}_{slip} & |\boldsymbol{f}_{stick}| > \mu F_n \\ \boldsymbol{f}_{stick} & \text{otherwise.} \end{cases} \tag{26}$$

A viscous term can be incorporated into this model as follows:

$$\boldsymbol{f}_{slip} = \boldsymbol{f}_{stick} \times \frac{\mu F_n}{|\boldsymbol{f}_{stick}|} - C_V \boldsymbol{V}_{clutch}\,, \tag{27}$$

which replaces Eq. (25). In this equation, C_V is the viscous friction parameter and $\boldsymbol{V}_{clutch}$ is the slipping velocity between the sphere and the ground.

3.1 Energy Audit

Energy dissipation due to friction force is the summation of the amount of dissipated energy by means of tangential dampers when the sphere is sticking on the ground, and the amount of energy dissipation by the clutch when the sphere is slipping.

Energy dissipation by the damper is calculated by

$$E_{TDamp} = \int_0^t D_t z^{\frac{1}{2}} \dot{u}^2\,\mathrm{d}t\,, \tag{28}$$

and energy dissipation by the clutch is

$$E_{Clutch} = \int_0^t \boldsymbol{F}_f \cdot \boldsymbol{V}_{clutch}\,\mathrm{d}t \tag{29}$$

where $\boldsymbol{V}_{clutch}$ is determined by

$$\boldsymbol{V}_{clutch} = \boldsymbol{V}_{sph} - \dot{\boldsymbol{u}}\,, \tag{30}$$

in which $\dot{\boldsymbol{u}}$ would be calculated by

$$\dot{\boldsymbol{u}} = \frac{\boldsymbol{F}_f + K_t z^{\frac{1}{2}} \boldsymbol{u}}{-D_t z^{\frac{1}{2}}}\,, \quad (z > 0). \tag{31}$$

In the sticking regime, the value of $\boldsymbol{f}_{stick}$ calculated by Eq. (22) ensures that

$$\dot{\boldsymbol{u}} = \boldsymbol{V}_{sph} \Rightarrow \boldsymbol{V}_{clutch} = \boldsymbol{0}\,, \tag{32}$$

which means that the clutch does not dissipate energy.

Also, the amount of energy stored in the tangential spring is

$$E_{TSp} = \int_0^t K_t z(t)^{\frac{1}{2}} u\, \dot{u}\, \mathrm{d}t\,. \tag{33}$$

4 Simulation of a Rolling Sphere

Equation of Motion

The motion equations for a rolling sphere on the ground in 3D space are

$$\boldsymbol{f} = m\ddot{\boldsymbol{c}} \tag{34}$$

and

$$\boldsymbol{n}_C = \bar{\boldsymbol{I}}_c\, \dot{\boldsymbol{\omega}} + \boldsymbol{\omega} \times \bar{\boldsymbol{I}}_c\, \boldsymbol{\omega}\,, \tag{35}$$

where $\boldsymbol{f}$ is the resultant force acting on the sphere, $\boldsymbol{n}_C$ is the moment around the center of the sphere, $\boldsymbol{c}$ is a vector giving the position of the center of mass, and $\boldsymbol{\omega}$ is the angular velocity of the sphere. The velocity of the contact point is calculated by

$$\boldsymbol{V}_P = \dot{\boldsymbol{c}} + \boldsymbol{\omega} \times \overrightarrow{CP}\,, \tag{36}$$

in which $\overrightarrow{CP}$ is a vector from the COM of the sphere to the contact point.

Also, for a rolling sphere, the energy of the body is calculated by

$$E_{Body} = mgh + \frac{1}{2} m \dot{\boldsymbol{c}}^2 + \frac{1}{2} \boldsymbol{\omega} \cdot \bar{\boldsymbol{I}}_c\, \boldsymbol{\omega}\,. \tag{37}$$

Results

Using MATLAB simulink, a simulation is done for a sphere with radius $r = 1.65$cm, mass $m = 154$gr, initial height of the center of mass 10cm, initial velocity in the x and y directions $= 0.5\frac{\mathrm{m}}{\mathrm{s}}$, $\mu = 0.2$, $C_V = 0.1$, $K_n = 8.5 \times 10^6$, $D_n = 3.1 \times 10^3$, $K_t = 12.75 \times 10^6$, $D_t = 3.1 \times 10^3$.

Figure 13 shows the friction force in the x direction. Because of the initial conditions, friction forces in both x and y directions are the same. Figure 14 shows the friction force in the x direction at the first bounce. It can be seen from this figure that the friction force is completely continuous and smooth. It is also shown that the contact starts with slipping of the sphere on the ground and after that as the normal force approaches its maximum value (according to Figure 10), the sphere sticks on the ground for less than 1ms and then again starts slipping until the end of the contact.

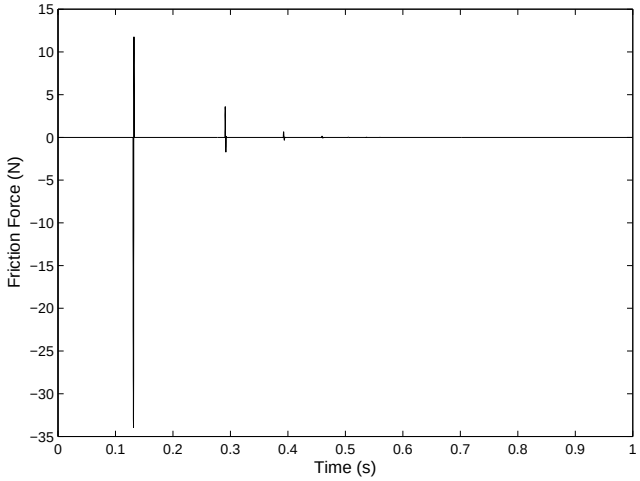

Figure 13: Friction force in x direction vs. time

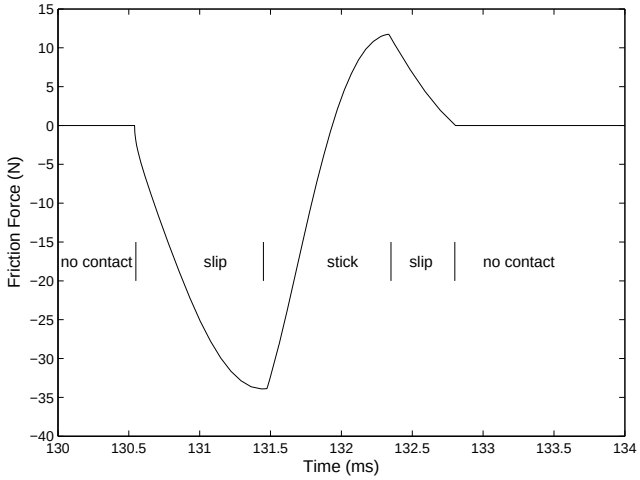

Figure 14: Friction force in x direction vs time for the first bounce of a sphere with radius 1.65cm which is released from the initial height 10cm

Figure 15 shows the x components of $\boldsymbol{c}$ and $\boldsymbol{V}_{sph}$ (i.e., the position of the COM and the velocity of the contact point). Looking at this figure, we can see that after 0.5s, the velocity is zero but the position is still increasing, which means that the sphere is rolling on the ground.

Figure 16 shows the total, damped, and stored energy during the rolling motion. As it should be, the amount of total energy is constant during the simulation and does not change.

5 Conclusion

A complete full 3D nonlinear contact model which is able to calculate both normal and friction forces is presented in this paper. A new nonlinear normal force model which is introduced in this paper is different from previous ones in the exponent of the ground deformation in the damp-

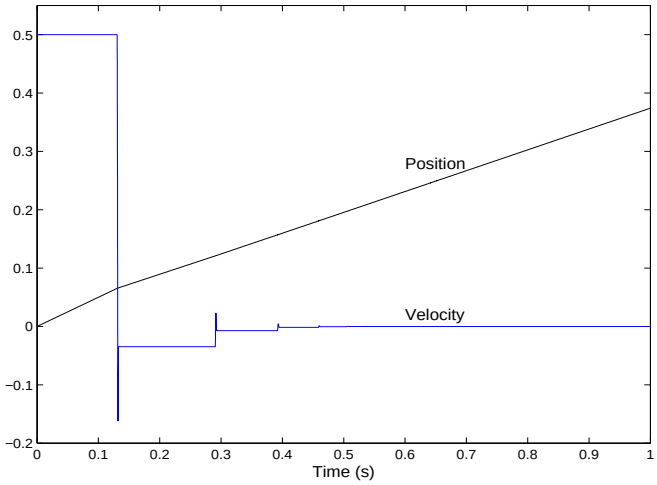

Figure 15: Position of the COM and velocity of the contact point in x direction

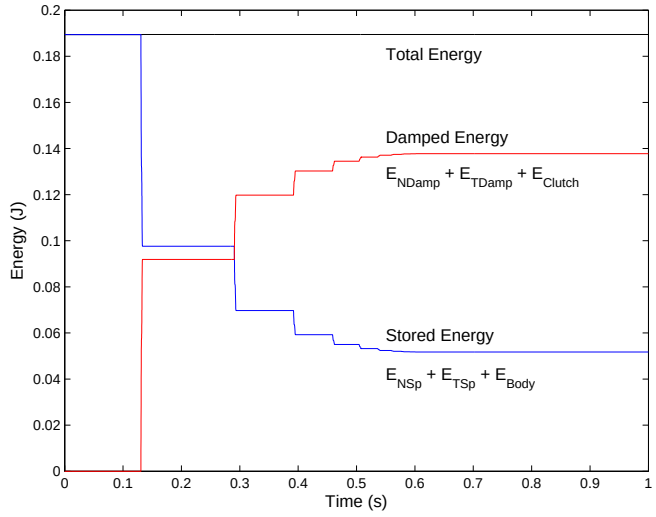

Figure 16: Energy vs time for a rolling sphere

ing term. The characteristics of this new model are also described. By comparing our results with the empirical results of the contact between a sphere and a plate, we showed that our model can predict values of the coefficient of restitution more accurately than the previous classical ones.

Also, a new nonlinear friction force model in two dimensions was presented in this paper, which is able to calculate pre-sliding displacement and viscous friction. This model uses a nonlinear equation for computing the friction force in stiction period.

Finally, rolling motion of a sphere on the ground was simulated and the results presented. As a non-spherical foot can be represented by a union of spheres, by using this model, it is possible to simulate the 3D motion of a robot's foot on the ground.

References

[Armstrong-Hélouvry *et al.*, 1994] B. Armstrong-Hélouvry, P. Dupont and C. C. de Wit. A survey of models, analysis tools and compensation methods for the control of machines with friction. *Automatica*, 30(7):1083–1138, 1994.

[Bliman and Sorine, 1995] P. A. Bliman and M. Sorine. Easy-to-use realistic dry friction models for automatic control. In *Proc. 3rd European Control Conference*, pages 3788–3794, Roma, Italy, September 1995.

[Dahl, 1968] P. Dahl. A solid friction model. Technical Report, The Aerospace Corporation, ElSegundo, CA, May 1968.

[de Wit *et al.*, 1995] C. de Wit, H. Olsson, K. J. Astrom and P. Lischinsky. A new model for control of systems with friction. *IEEE Trans. Automatic Control*, 40(3):419–425, 1995.

[Dupont *et al.*, 2000] P. Dupont, B. Armstrong and V. Hayward. Elasto-plastic friction model: contact compliance and stiction. In *Proc. American Control Conference*, pages 1072–1077, Chicago, Illinois, June 2000.

[Dupont *et al.*, 2002] P. Dupont, V. Hayward, B. Armstrong and F. Altpeter. Single state elastoplastic friction models. *IEEE Trans. Automatic Control*, 47(5):787–792, 2002.

[Falcon *et al.*, 1998] E. Falcon, C. Laroche, S. Fauve and C. Coste. Behavior of one inelastic ball bouncing repeatedly off the ground. *The European Physical Journal B*, 3:45–57, 1998.

[Featherstone, 2008] R. Featherstone. *Rigid body dynamics algorithms*. NewYork, USA: Springer, 2008.

[Gilardi and Sharf, 2002] G. Gilardi and I. Sharf. Literature survey of contact dynamics modelling. *Mechanism and Machine Theory*, 37:1213–1239, 2002.

[Goldsmith, 1960] W. Goldsmith. *Impact: the theory and physical behaviour of colliding solids*. London, U.K.: Edward Arnold, 1960.

[Haessig and Friedland, 1991] D. A. Haessig, Jr. and B. Friedland. On the modeling and simulation of friction. *J. Dynamic Systems, Measurement and Control*, 13:354–362, 1991.

[Hunt and Crossley, 1975] K. H. Hunt and F. R. E. Crossley. Coefficient of restitution interpreted as damping in vibroimpact. *J. Applied Mechanics*, 42(2):440–445, 1975.

[Johnson, 1977] K. L. Johnson. *Contact mechanics*. Cambridge University Press, 1977.

[Kuwabara and Kono, 1987] G. Kuwabara and K. Kono. Restitution coefficient in a collision between two spheres. *Japanese J. Applied Physics*, 26(8):1230–1233, 1987.

[Lankarani and Nikravesh, 1990] H. M. Lankarani and P. E. Nikravesh. A contact force model With hysteresis damping for impact analysis of multi-body systems. *J. Mechanical Design*, 112(3):369–376, 1990.

[Marhefka and Orin, 1999] D. W. Marhefka and D. E. Orin. A compliant contact model with nonlinear damping for simulation of robotic systems. *IEEE Trans. Systems, Man, and Cybernetics-part A: Systems and Humans*, 29(6):566–572, 1999.

[Olsson *et al.*, 1998] H. Olsson, K. J. Åström, C. C. de Wit, M. Gäfvert and P. Lischinsky. Friction models and friction compensation. *European J. Control*, 1998.